

RESEARCH

Open Access



Genome-wide identification and expression profiles of NAC transcription factors in *Poncirus trifoliata* reveal their potential roles in cold tolerance

Tian Fang¹, Yue Wang¹, Haowei Chen¹, Jing Qu¹, Peng Xiao¹, Yilei Wang¹, Xin Jiang¹, Chunlong Li^{1,2} and Ji-Hong Liu^{1,2*}

Abstract

Background Citrus, a globally vital economic crop, faces severe challenges due to extreme climatic conditions and diseases/pests attack. *Poncirus trifoliata* is closely related to citrus and shows unique cold tolerance, making it a crucial material for unraveling genes involved in cold tolerance. NAC (NAM, ATAF1/2, CUC2) transcription factors play important roles in plant growth, development, and stress responses. However, their evolution patterns and gene functions in citrus remain poorly studied. This study aims to elucidate the genomic characteristics and evolution of the NAC genes in *P. trifoliata*, and to analyze their expression patterns and conduct functional validation under cold stress.

Results Genome-wide analysis identified 135 *PtrNAC* genes in *P. trifoliata* with non-random chromosomal distribution, including 20 gene clusters. 57.78% of the NAC genes are located in the chromosomes 3, 4 and 5. Gene duplication analysis revealed that proximal and tandem duplications as primary expansion mechanisms, with tandem repeats specifically driving gene expansion in citrus lineages (subfamilies IV, V, and VII). Collinearity analysis showed that 24.44% of the *PtrNAC* genes were retained in homologous regions, and Ka/Ks ratio analysis further confirmed that purifying selection dominated their evolutionary process. Transcriptome landscapes revealed that *Pt5g024390* (*PtrNAC2*) was induced to the greatest degree under the cold stress. Meanwhile, expression level of *PtrNAC2* in tetraploid was more than two folds higher compared to diploid counterpart in the presence of cold stress. Virus-induced gene silencing of *PtrNAC2* led to significantly enhanced cold tolerance, implying that it plays a negative role in regulation of cold tolerance.

Conclusion This study systematically elucidated the global distribution and evolutionary patterns of NAC genes in *P. trifoliata*. In addition, the NAC gene exhibit adaptive expansion driven by tandem duplications. The identification of *PtrNAC2*, a negative regulator of cold tolerance in *P. trifoliata*, provides valuable insights into unravelling potential candidates for engineering cold tolerance in citrus.

*Correspondence:

Ji-Hong Liu
liujihong@mail.hzau.edu.cn

Full list of author information is available at the end of the article



© The Author(s) 2025. **Open Access** This article is licensed under a Creative Commons Attribution-NonCommercial-NoDerivatives 4.0 International License, which permits any non-commercial use, sharing, distribution and reproduction in any medium or format, as long as you give appropriate credit to the original author(s) and the source, provide a link to the Creative Commons licence, and indicate if you modified the licensed material. You do not have permission under this licence to share adapted material derived from this article or parts of it. The images or other third party material in this article are included in the article's Creative Commons licence, unless indicated otherwise in a credit line to the material. If material is not included in the article's Creative Commons licence and your intended use is not permitted by statutory regulation or exceeds the permitted use, you will need to obtain permission directly from the copyright holder. To view a copy of this licence, visit <http://creativecommons.org/licenses/by-nc-nd/4.0/>.

Keywords *Poncirus trifoliata*, NAC transcription factors, *PtrNAC2*, Genome-wide analysis, Tandem repeats, Cold tolerance

Background

Citrus, one of the most economically significant fruit tree crops globally, holds an irreplaceable position in the fruit industry and health sectors due to its nutritional value and processing properties. According to the USDA report [1], global citrus production in 2024 has declined due to extreme weather events (e.g., high temperatures, drought, frost) and disease outbreaks (e.g., Huanglong-bing), severely constraining sustainable development of the citrus industry and highlighting the urgency of breeding stress-resistant germplasms. Rootstock improvement represents a key strategy for enhancing citrus resilience to environmental stresses [2]. *Poncirus trifoliata*, known for its exceptional cold tolerance and broad-spectrum disease resistance and particularly for the enhanced stress resilience of its naturally autotetraploid variants (developed through natural polyploidization) compared to diploid counterparts [3, 4], has emerged as a pivotal material for deciphering stress adaptation mechanisms in woody plants. The release of its chromosome-level genome provides a critical tool for elucidating genome-environment interactions in perennial crops [5].

Plant molecular responses to environmental stresses involve multilayered gene regulatory networks, with transcription factors (TFs) playing central roles by orchestrating spatiotemporal expression of downstream targets [6–10]. The NAC (NAM, ATAF1/2, CUC2) TF family, one of the largest plant-specific regulatory protein families, exhibits functional diversity enabled by its conserved N-terminal DNA-binding domain and variable C-terminal transcriptional regulatory domain [11]. Since its initial discovery in *Petunia* [12], NAC TFs have been implicated in diverse biological processes, including organ development, senescence, and biotic/abiotic stress responses [13–15].

Recent advances highlight the pivotal regulatory roles of NAC TFs in stress adaptation. For example, in *Arabidopsis thaliana*, CLE14 activates *JUB1* to enhance reactive oxygen species (ROS) scavenging and delay senescence, while *JUB1* modulates gibberellic acid (GA) and brassinosteroids (BR) signaling to strengthen stress resilience through interconnected transcriptional and peptide networks [16–18]. *ANAC070* improves aluminum tolerance by suppressing the *ANAC017-XTH31* pathway in *A. thaliana* [19]. In rice (*Oryza sativa* L.), *OsNAC42* enhances nitrogen use efficiency via nitrate uptake regulation [20], while *OsNAC5* activates *OsABI5* to confer cold tolerance [21]. *OsNAC023* interacts with *OsREM1.5* under stress, translocating to the nucleus to activate drought/heat-responsive pathways [22]. In

tomato (*Solanum lycopersicum* L.), the *miR164a*-*NAM3* module and *SINAP1* improve stress tolerance and fruit yield by balancing phytohormones [23, 24]. In woody species, *MdNAC104* enhances apple cold tolerance through CBF-dependent and -independent pathways [25], while citrus *PtrNAC72* negatively regulates drought resistance by suppressing putrescine biosynthesis [26]. *CrNAC036* and *CrMYB68* synergistically delay fruit ripening by repressing *NCED5*-mediated abscisic acid (ABA) synthesis [27]. Anthocyanins play an important role in resisting biotic and abiotic stresses, *PpNAC1* was essential for enhancing anthocyanin biosynthesis [28]. These findings underscore NACs as central hubs in plant stress regulatory networks.

Despite comprehensive genomic analyses of NACs in multiple plant species [29–33], systematic insights into their evolution, functional diversification, and cold-responsive networks in *P. trifoliata* remain lacking. These knowledge gaps hinder both mechanistic understanding of woody plant stress adaptation and NAC-based molecular breeding in citrus. In this study we performed genome-wide characterization of the NAC family in *P. trifoliata*. By integrating comparative genomics and transcriptomics, we reveal lineage-specific expansion patterns driven by tandem duplication, elucidate cold-induced expression patterns of the NAC genes. In addition, we employed virus-induced gene silencing (VIGS) to investigate the functions of the cold-inducible genes in regulation of cold tolerance. These findings establish a framework for deciphering complex stress adaptation mechanisms in citrus and may hold promise for molecular breeding of cold-tolerant citrus.

Materials and methods

Plant materials and cold treatment

Four citrus genotypes were selected: *P. trifoliata*, *Citrus ichangensis* Swingle, *C. grandis*, and *C. limon*. Seeds provided by the Citrus Breeding Center of Huazhong Agricultural University were sown in plastic pots containing commercial substrate (peat: vermiculite: perlite = 3:1:1, v/v/v). Plants were cultivated in growth chambers under controlled conditions (25 °C, 60–70% RH, 16 h / 8 h photoperiod) for three months. Uniform healthy seedlings were subjected to cold treatment (4 °C), with sampling at 0 h, 6 h, 24 h, 72 h and after 48 h recovery. The leaf samples containing three biological replicates with pooled leaves from five plants, were frozen in liquid nitrogen and stored at -80 °C.

Genomic data collection and processing

Genomic data, including coding sequences (CDS), protein sequences, gene structure annotations (GFF3), and genome sequences, were obtained from two databases. The Citrus Pan-Genome Breeding Database (CPBD, <http://citrus.hzau.edu.cn/>) [5, 34–42], and the JGI Data Portal (<https://data.jgi.doe.gov/>) provides access to reference datasets for *A. thaliana* [43]. A standardized workflow was applied to generate unified datasets for each species, containing the longest protein sequences, longest CDS sequences, filtered gene structure annotations, and genome sequences. For CPBD data: Python scripts were developed to select the longest transcript isoforms, and Perl scripts were used to clean the annotation files. For JGI data: File consistency was verified, redundant suffixes in GFF3 annotations were removed, and the longest transcripts were extracted. Additionally, due to structural complexity, three genes in *P. trifoliata* (*Pt3g017300*, *Pt4g010630*, *Pt7g019640*) were re-annotated using GSAman.

Identification and characterization of NAC genes

The *A. thaliana* NAC gene reference dataset was compiled using the PlantTFDB (<https://planttfdb.gao-lab.org/>) [44] and TAIR (<https://www.arabidopsis.org/>) [45] databases. The hidden Markov model (HMM) for the NAC conserved domain (PF02365) was obtained from the Pfam database (<http://pfam.xfam.org/>) [46]. To establish the *A. thaliana* NAC gene family dataset, candidate sequences were initially retained through HMM scans or BLAST homology searches [47]. The presence of the NAM domain in these candidate sequences was subsequently confirmed using the SMART database (<http://smart.embl.de/>) [48]. To identify NAC genes in other species using the *A. thaliana* dataset, genes recognized by both HMM searches (E-value threshold: $1e-5$) and BLASTP (E-value $< 1e-5$, sequence similarity $> 30\%$) were retained. The NAM domain was further validated using the SMART database. Physicochemical properties of the confirmed NAC proteins, such as molecular weight and isoelectric point, were analyzed using the Peptides package in R [49]. Subcellular localization predictions were conducted with WoLF PSORT (<https://wolfsort.hgc.jp/>) [50].

Phylogenetic analysis

Multiple sequence alignment was performed using MUSCLE software to identify conserved domains and residues [51]. A phylogenetic tree was constructed with IQ-TREE, and its reliability was tested using 1,000 bootstrap replicates [52]. SNPs from four-fold degenerate sites were used to build the tree. The maximum likelihood tree was generated with RAxML software under the GTRGAMMA model [53]. *Atalantia buxifolia* was

selected as the outgroup, and 100 bootstrap analyses were conducted to evaluate node support. High-resolution phylogenetic visualizations were created using the Interactive Tree of Life (iTOL) platform (<https://itol.embl.de/>) [54].

Analysis of gene structure, conserved motifs, and cis-acting elements

Conserved protein motifs were identified using the MEME tool (10 conserved motifs spanning 6–100 amino acids). Gene structure organization was analyzed by systematically examining exon-intron boundaries and untranslated regions (UTRs) based on genome annotation data. The 2,000-bp promoter sequences upstream of *PtrNAC* genes were extracted using the “Sequence Retrieval” tool from the Citrus Pan-Genome Breeding Database. Cis-acting elements in these sequences were predicted using PlantCARE (<https://bioinformatics.psb.ugent.be/webtools/plantcare/html/>) [55]. The Gene Structure Display Server (GSDS, <http://gsds.cbi.pku.edu.cn>) was employed to generate visual representations of all analyses, which were integrated with phylogenetic data [56].

Genomic collinearity and evolutionary analysis

Protein sequence alignment was performed using BLASTP (E-value $\leq 1e-10$). Gene duplication patterns, including tandem duplications and collinear regions, were identified with MCScanX [57]. Circular genome visualization was generated using Circos [58], while linear chromosomal maps were constructed with MG2C_v2.1 [59]. Sequence alignment was conducted via MUSCLE, and Ka/Ks ratios were calculated using KaKs_Calculator [60]. In the collinearity analysis, protein sequence similarity was first evaluated using BLAST (E-value $\leq 1e-10$, maximum 5 target sequences). Subsequently, collinear regions between genomes were identified using MCScanX. Finally, data were processed and visualized through the JCVI toolkit (filtering criteria: minspan = 10).

RNA isolation and gene expression profiling

Total RNA was extracted using the RNA extraction kit (RN33; Aidlab Biotech Co. Ltd, Beijing, China) and reverse-transcribed into cDNA with HiScript III RT SuperMix for RT-qPCR (+gDNA wiper) (Vazyme, Nanjing, China). Quantitative PCR was performed on an ABI7500 system (Applied Biosystems, Foster City, CA, USA) using AceQ SYBR Green Master Mix (Vazyme, Nanjing, China). The RT-qPCR protocol consisted with initial denaturation step at 95 °C for 5 min, this was followed by 40 cycles of three steps: 95 °C for 10 s, 60 °C for 30 s, and 95 °C for 15 s. After cycling, final steps were performed at 60 °C for 60 s and 95 °C for 15 s. Each 10 μ L reaction mixture contained 5 μ L of 2 \times SYBR Green PCR

Master Mix, 0.2 µL of 10 mM primers, and 200 ng cDNA template. Relative expression levels were calculated using the $2^{-\Delta\Delta C_T}$ method with *ACTIN* as the reference gene [61]. Three biological replicates were performed. Gene-specific primer sequences are listed in Table S1. Data visualization was completed using Microsoft Excel.

Virus-induced gene silencing (VIGS)

The function of the *PtrNAC2* gene was investigated using VIGS. A 280-bp fragment of *PtrNAC2* was amplified using primers containing *Bam*HI and *Sma*I restriction sites and cloned into the pTRV2 vector to construct pTRV2-*PtrNAC2*. Gene-specific primer sequences are listed in Table S2. Recombinant plasmids were introduced into *Agrobacterium* GV3101 via heat shock transformation. The pTRV2-*PtrNAC2* (or pTRV2 control) was mixed with pTRV1 at a 1:1 ratio and infiltrated into one-month-old *P. trifoliata* seedlings for VIGS experiments [62, 63]. Infected plants were incubated at 25 °C in darkness for 72 h, then transferred to soil for one month. Positive transgenic lines were screened by genomic PCR, and RT-qPCR was used to quantify *PtrNAC2* transcript levels to verify silencing efficiency.

Cold tolerance assay and physiological measurements

VIGS-silenced and control plants were exposed to -4 °C for 8 h, when the difference in cold tolerance between the tested group was obvious. Leaf samples were immediately collected for physiological analysis. Membrane integrity was evaluated by measuring electrolyte leakage [64]. Photosynthetic efficiency was assessed using an IMAGING-PAM chlorophyll fluorometer (Walz, Germany), and the maximum quantum yield of PSII (*Fv/Fm*) was calculated with Imaging Win Gege software [65].

Data analysis methods

Statistical analysis was performed using SPSS software (v22.0). Differences between treatment groups were tested by one-way ANOVA with LSD post hoc tests. Significance levels were set at $P < 0.05$ (*), $P < 0.01$ (**), and $P < 0.001$ (***)

Results

Genome-wide identification and physicochemical properties analysis of NAC genes

In this study, we systematically identified and characterized the NAC transcription factor family in *P. trifoliata* using a rigorously validated *A. thaliana* NAC gene dataset (118 members, Table S3), which included five genes with transcript variants: *AT1G56010.1/AT1G56010.2*; *AT2G02450.1/AT2G02450.2* *AT2G24430.1/AT2G24430.2*; *AT3G10490.1/AT3G10490.2* and *AT5G07680.1/AT5G07680.2*. A total of 135 *PtrNAC* members were identified, including four pairs of identical

sequences: *Pt5g023950.1/Pt5g025720.1*; *Pt9g021720.1/PtUn031790.1*; *PtUn023510.1/Pt5g024390.1* and *Pt4g011620.1/Pt4g011640.1*. These duplications may result from gene duplication events, genome assembly redundancy, or annotation errors. To ensure data integrity, all paralogous genes were retained for subsequent evolutionary analysis. Notably, three structurally complex NAC genes (*Pt3g017300.1*, *Pt4g010630.1*, *Pt7g019640.1*) required re-annotation using the GSaman tool to resolve annotation discrepancies.

Physicochemical analysis showed varied properties among *PtrNAC* proteins (Table S4). Protein lengths differed from 114 to 1,184 amino acids, with most between 300 and 500 residues. Molecular weights ranged 13.4–130.7 kDa, mainly falling in 30–50 kDa. Isoelectric points spanned 4.04 to 10.12, covering acidic to alkaline ranges. Nuclear localization dominated predictions (74.8%), matching typical regulatory functions. Other proteins appeared in cytoplasm (9.6%), peroxisomes (5.9%), chloroplasts (3.7%), cell membranes (3.7%), mitochondria (1.5%), and Golgi (0.7%), suggesting functional diversification beyond nuclear activities.

Chromosomal location and distribution of the NACs

Genomic analysis revealed a unique chromosome patterns of NAC genes in *P. trifoliata* (Fig. 1; Table S5). Of 135 *PtrNAC* genes, 121 (89.6%) mapped to nine chromosomes (Chr1–Chr9), exhibiting a non-random distribution pattern. Chr5 (28 genes, 20.74%), Chr3 (27 genes, 20.00%), and Chr4 (23 genes, 17.04%) together contained 57.78% of genes. Chr7 (1 gene, 0.74%) and Chr8 (3 genes, 2.22%) had the least number of genes. Further analysis identified 20 gene clusters (intergenic spacing ≤ 50 kb) showed structural variety. The largest cluster (10 genes/135.5 kb) was observed on Chr5 (*Pt5g023870-Pt5g023980*). Smaller clusters held 2–4 genes. Notably, the Chr2 cluster exhibited the smallest average spacing (989 bp; minimum spacing: 714 bp), and gene overlap was observed between *Pt3g034550* and *Pt3g034560* on Chr3. Chromosome-specific distribution patterns were prominent: four genes in the *Pt4g011610-Pt4g011650* region of Chr4 displayed highly regular clustering (spacing: 3,861–3,873 bp), Chr5 and Chr4 each contained four high-density clusters, and Chr3 harbored three tightly linked cluster groups. Importantly, three small clusters (14 genes, 10.37%) remained on unanchored genomic scaffolds (designated ChrUn), potentially reflecting gaps in the current genome assembly or unresolved structural complexities in these regions. Genome-wide cluster spacing showed extreme variation (ranging from 714 bp to 38.4 kb, with an average of 11.3 kb). The tandem duplication-dominated distribution pattern (e.g., the largest cluster on Chr5) and clustered amplification of functionally related genes suggest that NAC family evolution may

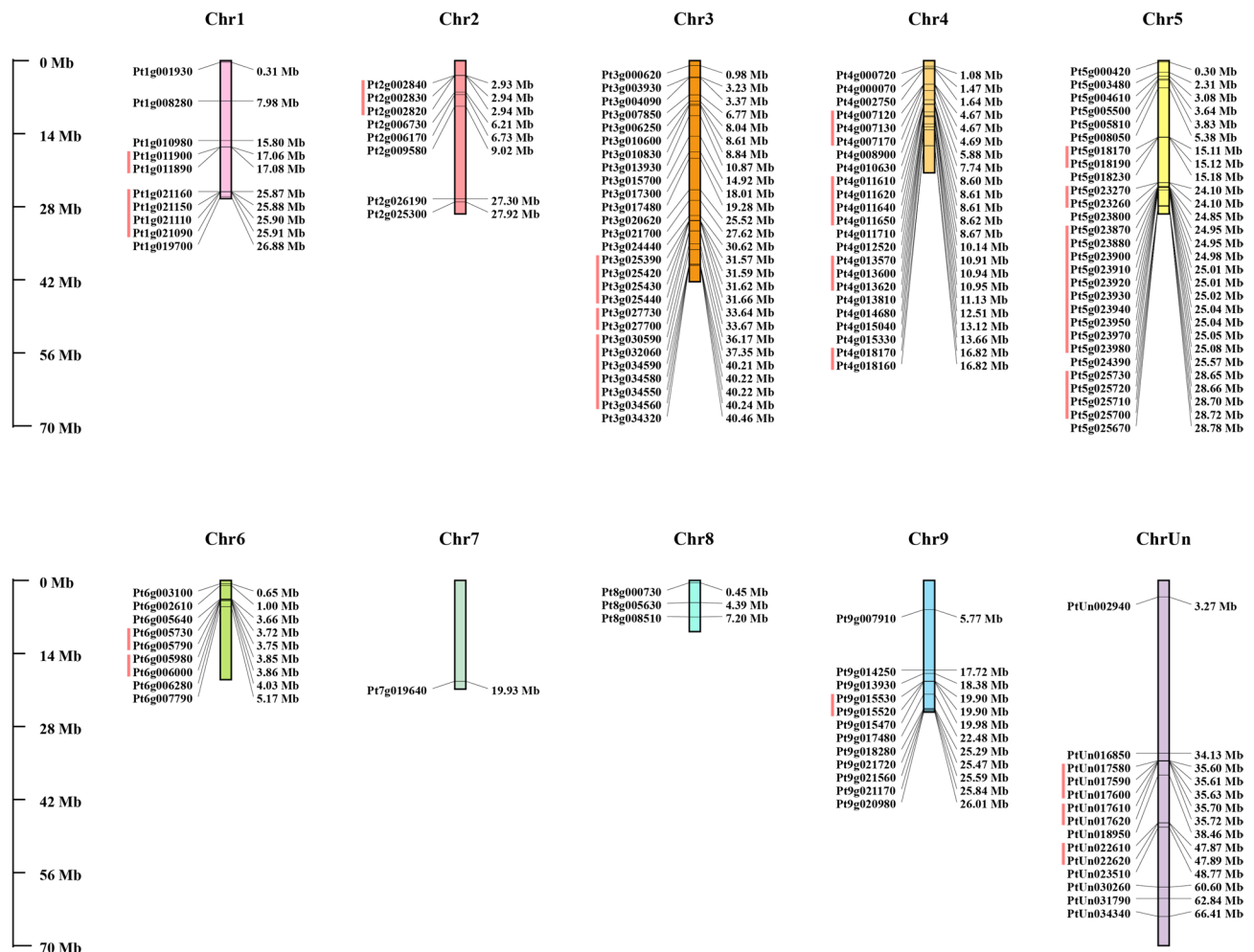


Fig. 1 Schematic representations for the chromosomal distribution of *P. trifoliata* NACs. In chromosomal ideogram representation, genomic annotations are bifurcated along the axis: Gene identifiers (IDs) are systematically displayed on the left flank, while corresponding physical positions along the chromosome are precisely mapped on the right flank. Gene clusters localization is indicated by a vertical red bar located to the left of gene identifiers

be driven by localized duplication events and regulated by chromosome-specific recombination mechanisms.

Phylogenetic classification and subfamily dynamics of NAC proteins

Phylogenetic analysis revealed distinct evolutionary patterns of the NAC gene family between *A. thaliana* and *P. trifoliata*. A phylogenetic tree was constructed based on conserved domains. The 118 *Arabidopsis* NAC members divided into seven evolutionary groups (I-VII) with these distributions: Group I: 17 members (14.41%); Group II: 13 members (11.02%); Group III: 9 members (7.63%); Group IV: 19 members (16.10%); Group V: 23 members (19.49%); Group VI: 25 members (21.19%); Group VII: 11 members (9.32%). In contrast, the 135 *PtrNAC* genes in *P. trifoliata* exhibited significant distribution shifts: Group IV (27 genes, 20.00%), Group V (37 genes, 27.41%), and Group VII (29 genes, 21.48%) showed marked expansion, while Group I (10 genes, 7.41%) and Group II (8 genes,

5.93%) displayed relative contraction (Fig. 2; Table S6). Notably, lineage-specific subclades containing 29, 10, and 23 members were identified in Group V, VI, and VII of *P. trifoliata*, respectively, suggesting potential functional innovation events during citrus lineage evolution.

Analysis of domain composition and conserved motifs

Systematic analysis of 135 *PtrNAC* proteins revealed distinct features in domain composition and conserved motifs (Fig. 3). Domain analysis showed that 97.8% (132/135) of members contained a single conserved NAM domain, consistent with the canonical characteristics of the NAC family. Three atypical members (*Pt5g023900*, *Pt9g021560*, *PtUn022620*) harbored dual NAM domains, while partial members (e.g., *Pt4g010630*) exhibited NAM domains specifically localized at the C-terminus. Eleven additional functional domains were identified, including RRM_SF in *Pt5g005810* and KTI12 in *Pt4g007170*, indicating potential functional

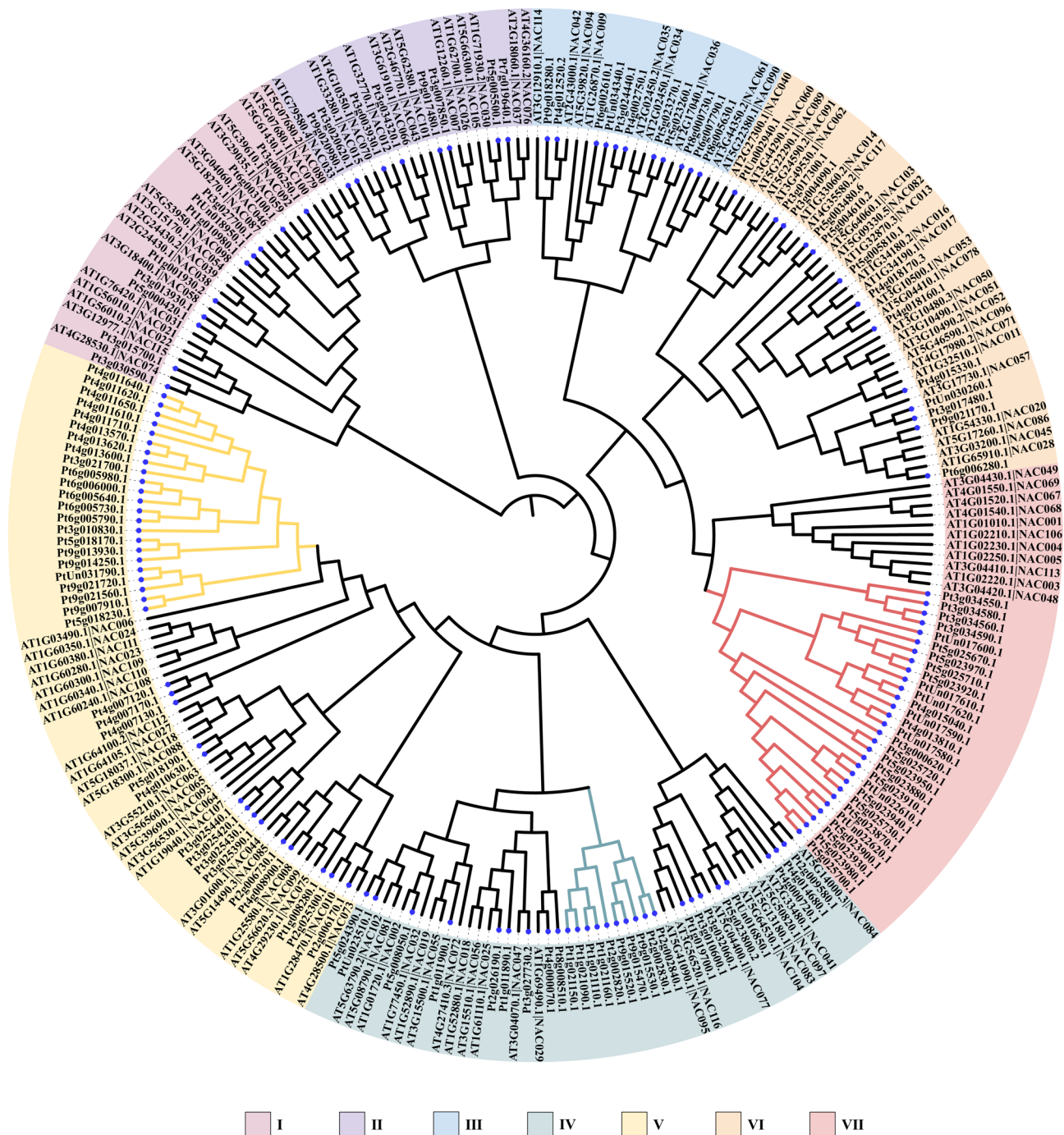


Fig. 2 Classification and phylogenetic analysis of *PtrNAC* genes. Phylogenetic topology-based clustering classified the gene family members into seven evolutionary clades (designated as Group I-VII) with distinct color coding; *P. trifoliata* NAC genes were distinctively highlighted using azure circular markers

divergence. MEME motif prediction identified 10 significant conserved motifs (Table S7): Motifs 1–7 were highly conserved (coverage: 64.4–96.3%; occurrence: 90–136 times), with spatial distributions overlapping the NAM domains. In contrast, Motifs 8–10 showed lineage-specific distribution (Group VII), with lower coverage (15.6–18.5%) and occurrence (24–58 times), potentially involved in subfunctional differentiation. Phylogenetic

analysis revealed conserved motif combination patterns within evolutionary clades. For example, Motifs 1-2-3-4 formed a core cluster in most proteins, and tandem motif arrangements (e.g., Motif pairs 1-2 and 5-6) frequently occurred, suggesting functional synergy. Gene structure analysis demonstrated significant variation in exon numbers (1-16), with 11.85% (16/135) of members completely lacking introns. Phylogenetic clustering divided

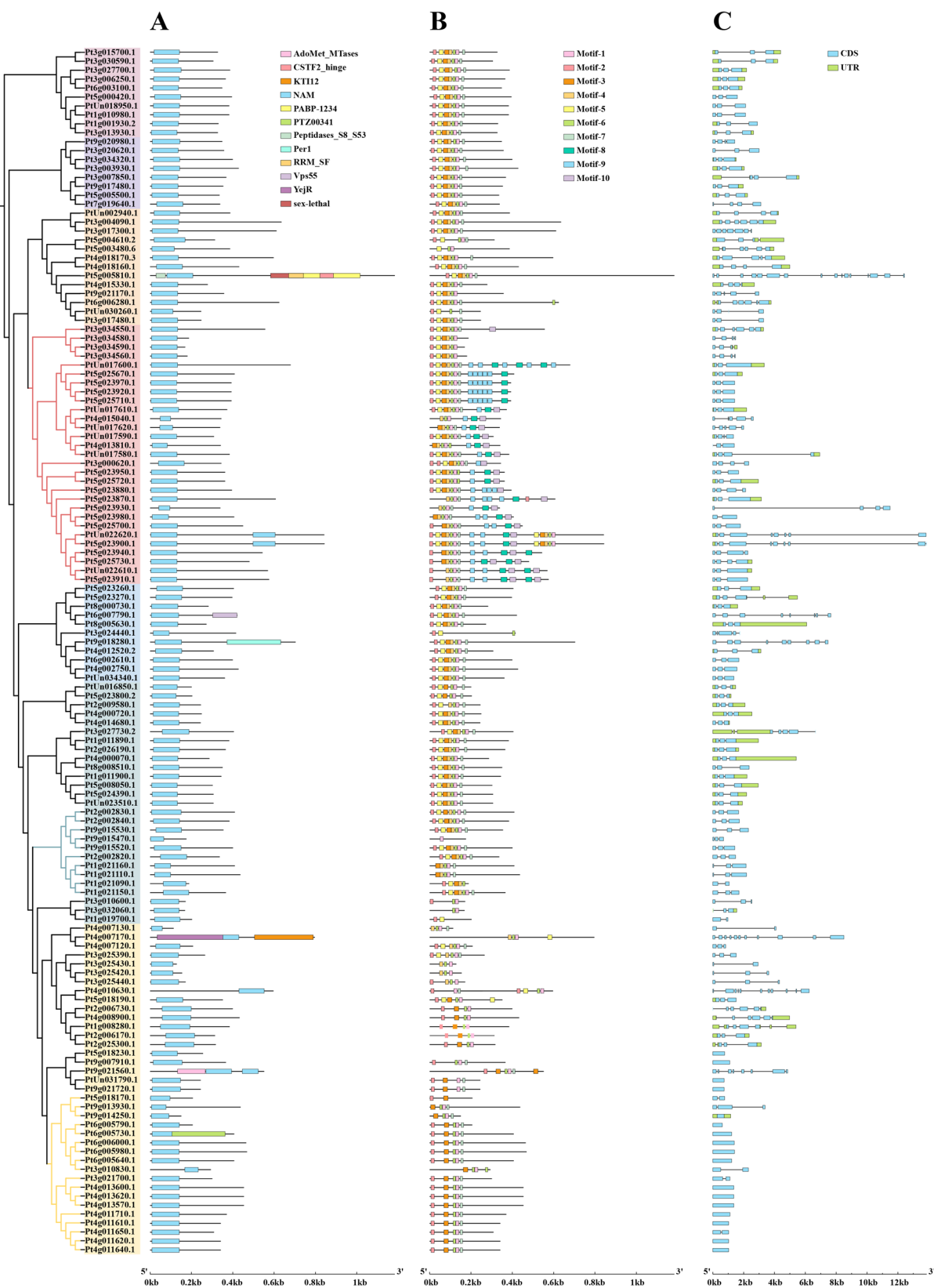


Fig. 3 (See legend on next page.)

(See figure on previous page.)

Fig. 3 Structural and conserved motif analysis of *PtNAC* genes. **(A)** Conserved domains of *PtNAC* proteins. Twelve conserved domains are displayed as boxes in different colors. **(B)** Motif composition of *PtNAC* proteins. Ten motifs are shown as boxes in different colors. Detailed motif sequences are described in Supplementary Table S7. **(C)** Structure of *PtNAC* genes. Green boxes denote the 5'/3' untranslated regions (UTRs), blue boxes indicate coding sequences (CDS), and black connector lines indicate introns. Genomic scale information can be converted to nucleotide measurements using the scale bar at the bottom

the family into seven subfamilies, where Group VII members generally possessed complex gene structures (exons ≥ 10). Notably, phylogenetically adjacent members (e.g., *Pt5g023870.1* and *Pt5g023900.1*) displayed conserved exon-intron arrangements, suggesting potential functional correlations.

Analysis of promoter *cis*-acting elements

Systematic analysis of promoter regions (2,000 bp upstream of the ATG start codon) in 135 *P. trifoliata* NAC genes identified 83 types of *cis*-acting elements, classified into four major functional categories (Fig. 4). The first group was stress-responsive elements, encompassing ARE (anaerobic induction), TC-rich repeats (defense stress), WUN-motif (wound response), and MBS (drought response). The second group was hormone-responsive elements, including ABRE (abscisic acid response), TGA-element (salicylic acid response), GARE-motif (gibberellin response), and TGACG-motif (jasmonic acid response). The third group was light-responsive elements, predominantly distributed Box 4, supplemented by frequently occurring G-box and I-box, indicating the potential role of light signaling in NAC gene regulatory networks. The last group was growth and development-related elements, including AAGAA-motif (regulating endosperm expression), CAT-box (meristem-specific expression), and O₂-site (storage protein synthesis regulation). Notably, MYB and MYC-recognizing elements, closely associated with abiotic stress, were widely distributed across the family. The enrichment of hormone- and stress-responsive elements in the promoter regions suggests that the *P. trifoliata* NAC gene family may regulate plant environmental adaptation through complex transcriptional networks.

Analysis of genome duplication patterns

Analysis of 25,680 genes showed different duplication patterns in the *P. trifoliata* genome. Gene duplication modes were ranked by prevalence as follows: dispersed duplication (41.48%, 10,653 genes) predominated, followed by whole-genome/segmental duplication (19.96%, 5,125 genes), singleton duplication (16.78%, 4,309 genes), tandem duplication (12.73%, 3,268 genes), and proximal duplication (9.05%, 2,325 genes). Notably, the NAC transcription factor family (135 genes) exhibited a unique duplication profile: dispersed duplication (34.07%, 46 genes) and whole-genome/segmental duplication (25.19%, 34 genes) constituted the primary modes,

followed by tandem duplication (20.74%, 28 genes) and proximal duplication (18.52%, 25 genes), while singleton duplication (1.48%, 2 genes) showed minimal representation (Table S8).

Analysis of collinearity and selection pressure

Whole-genome collinearity analysis identified 233 collinear regions encompassing 5,125 genes (19.96% of total genes), with 2,148 tandem duplicate genes involving 3,697 genes. Within the NAC family, 20 collinear gene pairs (involving 33 *PtNAC* genes) were identified, representing 24.44% of this family (Fig. 5). Ka/Ks analysis revealed strong purifying selection in 17 gene pairs (Table S9), with ratios ranging from 0.051 to 0.330. Notably, the pair *Pt1g010980-PtUn018950* showed absence of nonsynonymous substitutions (Ka = NA), preventing ratio calculation, while *Pt5g024390-PtUn023510* and *Pt9g021720-PtUn031790* exhibited identical sequences. These findings demonstrate that purifying selection predominates in NAC family evolution while maintaining dynamic equilibrium through local functional differentiation.

Analysis of evolutionary differentiation and subfamilies in citrus genus

Phylogenetic analysis revealed dynamic evolutionary characteristics of the NAC gene family in citrus during speciation (Fig. 6, Table S10). Basal lineages included *A. buxifolia* (127 members), *P. trifoliata* (135 members), and *C. ichangensis* (141 members). Subfamily differentiation showed marked heterogeneity: Subfamily VII displayed the highest evolutionary plasticity, with member counts sharply decreasing from 22–33 in early lineages to 0–1 in *C. medica* and *C. grandis* 'Huazhou'; Subfamily IV peaked in *Fortunella hindsii* (43 members), while Subfamily V expanded significantly in *C. grandis* 'Wanbai' (cultivar, 55 members); Subfamilies I, II, III, and VI maintained stable member counts (9–10, 7–11, 10–15, and 10–13, respectively). Notably, cultivated pummelo lineages demonstrated a distinct lineage-specific expansion pattern—a stepwise increase from *C. grandis* 'Huazhou' (63 members) through *C. grandis* 'Majia' (109 members) to *C. grandis* 'Wanbai' (126 members)—closely aligned with domestication stages, suggesting adaptive genomic restructuring potentially driven by artificial selection pressure.

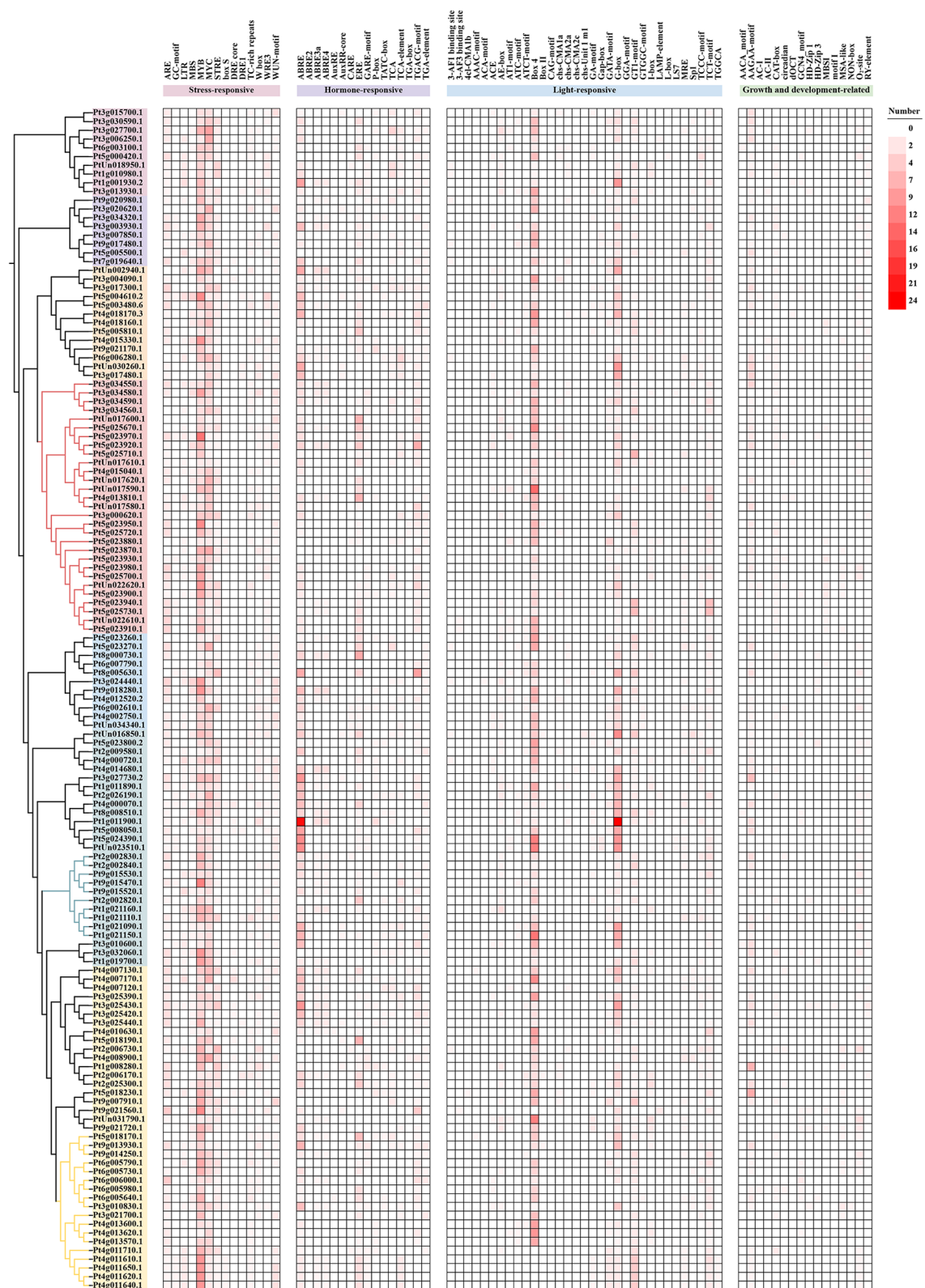


Fig. 4 *Cis*-acting elements in the promoters of *PtrNAC* genes. The *cis*-acting elements were divided into four functional categories: stress-responsive elements, hormone-responsive elements, light signaling elements, and growth and development regulation elements. Element quantity differences are displayed through a red-scale gradient

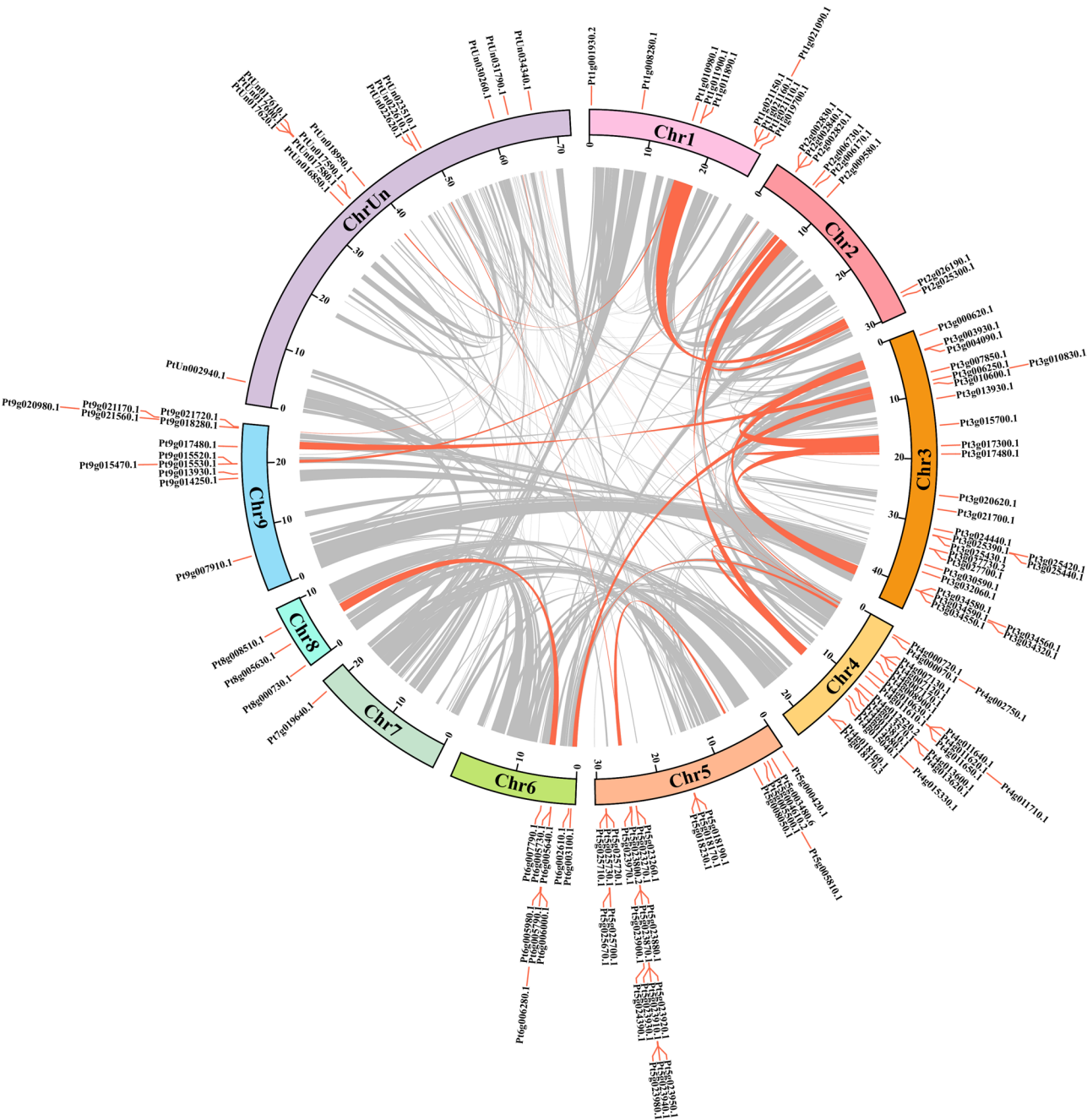


Fig. 5 Collinearity analysis of the *PtrNAC* genes. In the circular genome alignment diagram, gray connecting arcs indicate genome-wide syntenic regions, while orange connecting bands specifically highlight conserved homologous regions containing *PtrNAC* genes. The peripheral radial layout illustrates the linear distribution pattern of *P. trifoliata* NAC gene family members along chromosomes, with a chromosomal scale ring providing megabase (Mb)-level physical position references

Analysis of species collinearity

Collinearity analysis was conducted using *P. trifoliata* as the reference genome. The results showed a non-linear evolutionary trend in conserved NAC gene homologs across citrus species (Fig. 7; Table S11). In evolutionary timelines, the early-diverging species *C. ichangensis* (62 NAC regions) and the terminal taxa *C. grandis* ‘Majia’ (62) and *C. grandis* ‘Wanbai’ (62) exhibited the highest

values. In contrast, early-stage species *A. buxifoliata* (46) and mid-diverging species *C. sinensis* (47) and *C. reticulata* (48) showed significant reductions. Notably, *C. medica* (53), a late-diverging species, retained fewer conserved regions than the early-diverging *C. ichangensis*, suggesting that the conservation of this gene family may be driven by ecological adaptation rather than strictly following phylogenetic timelines. Whole-genome

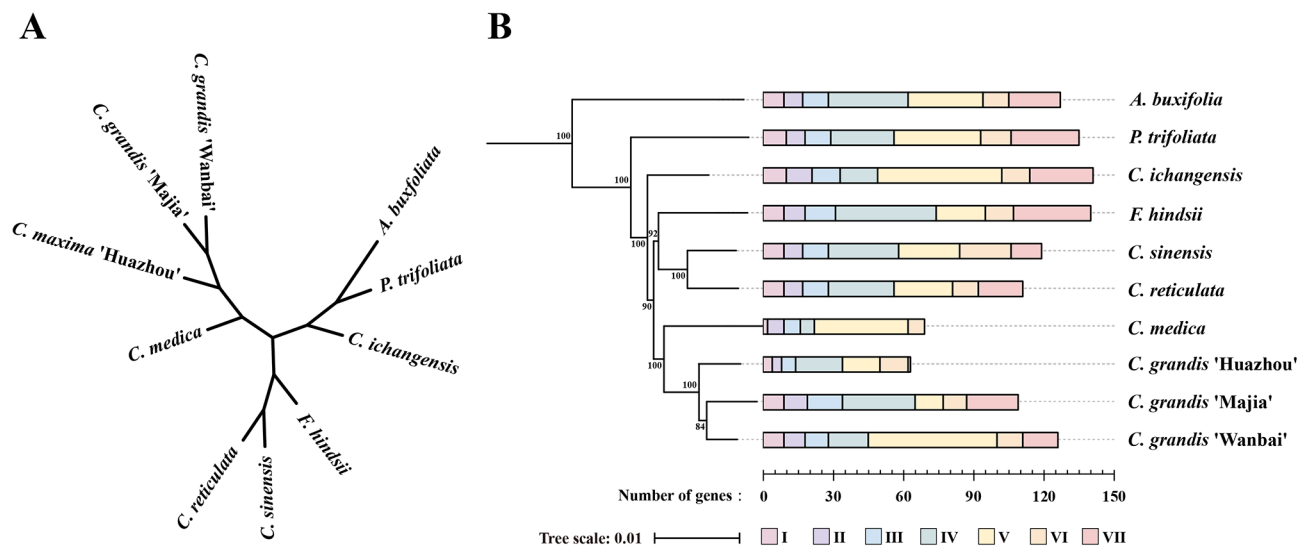


Fig. 6 Phylogenetic tree of citrus and analysis of subfamily divergence in the NAC gene family during citrus evolution. **(A)** Phylogenetic tree depicting the phylogenetic relationships among citrus species. **(B)** Distribution of NAC gene subfamilies within citrus. Branch lengths indicate genetic divergence

collinearity analysis indicated a stepwise increase in the number of syntenic genes from early-diverging *A. buxifolia* (624) to late-diverging *C. grandis* 'Majia' (697). However, *C. medica* (556 genes) deviated significantly, showing a sharp decline of 11% compared to its closely related species *C. grandis* 'Huazhou' (625). The gene density (total genes/syntenic regions) remained highly conserved across all species (~50 genes per region), reflecting strong stability in gene distribution patterns within syntenic regions during evolution. Of particular note, *C. grandis* 'Majia' and *C. grandis* 'Wanbai' possessed the highest numbers of syntenic regions (697 and 672, respectively) and conserved NAC regions (both 62), likely due to artificial domestication favoring genetic stability.

Expression patterns of *PtRNACs* under cold stress

Transcriptomic analysis of cold (0 h, 6 h, 24 h, 72 h) stress responses in *P. trifoliata* revealed significant evolutionary and functional divergence within the NAC transcription factor family (Fig. 8). Phylogenetic analysis identified stress-responsive genes (e.g., *Pt1g011900*, *Pt4g000070*, *Pt5g008050*, *Pt5g024390*) forming a distinct clade, showing strong induction under cold stresses. *Pt1g011900* exhibited a 2.1-fold increase at 6 h of cold stress, escalating to 26.1-fold by 72 h. Similarly, *PtRNAC2* showed rapid induction with a 10.1-fold increase at 6 h and a 25.6-fold peak at 72 h under cold stress. The temporal expression patterns of these genes correlated with their phylogenetic clustering, indicating their central role in citrus stress adaptation. In contrast, genes like *Pt2g009580* displayed marked suppression, with a 63.7% decrease under cold stress. Constitutively expressed genes (e.g., *Pt2g025300*) kept similar levels under cold treatments, suggesting

roles in basal metabolic regulation. This tripartite functional divergence—inducible, suppressive, and constitutive—reflects the NAC family's strategic diversity in environmental adaptation.

Analysis of germplasm-specific expression and dosage effect regulation

To systematically elucidate the regulatory mechanisms of NAC transcription factors in citrus cold adaptation, this study integrated transcriptomic data and RT-qPCR validation from different citrus germplasm types (wild, cultivated, and polyploid materials). Four core NAC genes (*Pt1g011900*, *Pt4g000070*, *Pt5g008050*, *Pt5g024390*) showed significant cold-induced expression but with distinct dynamic patterns across germplasms.

In *C. ichangensis* vs. *C. limon* comparisons, basal expression levels of *C. ichangensis* genes were generally higher than those of *C. limon*, with stronger cold induction (Fig. 9A). For example, homologous gene *Pt1g011900* in *C. ichangensis* reached 1,771.88, 4.1-fold higher than *C. limon*, consistent with its stronger cold adaptation capacity. Comparisons of the expression levels in the wild mandarin (*C. reticulata*) and cultivated species 'Ponkan' revealed that the wild species exhibited lower basal expression but was significantly induced under the cold stress (Fig. 9B), suggesting that the wild species may enhance environmental responsiveness for adaptive advantages. In tetraploid vs. diploid *P. trifoliata*, cold stress markedly altered genomic dosage effects: the tetraploid/diploid expression ratio under normal conditions was near 1:1, but increased to 2.5:1 after 72 h cold treatment. All tested genes showed positive dosage effects (mean ratio 2.15 ± 0.32) (Fig. 9C). Notably, *PtRNAC2* displayed the strongest cold induction. In *C.*

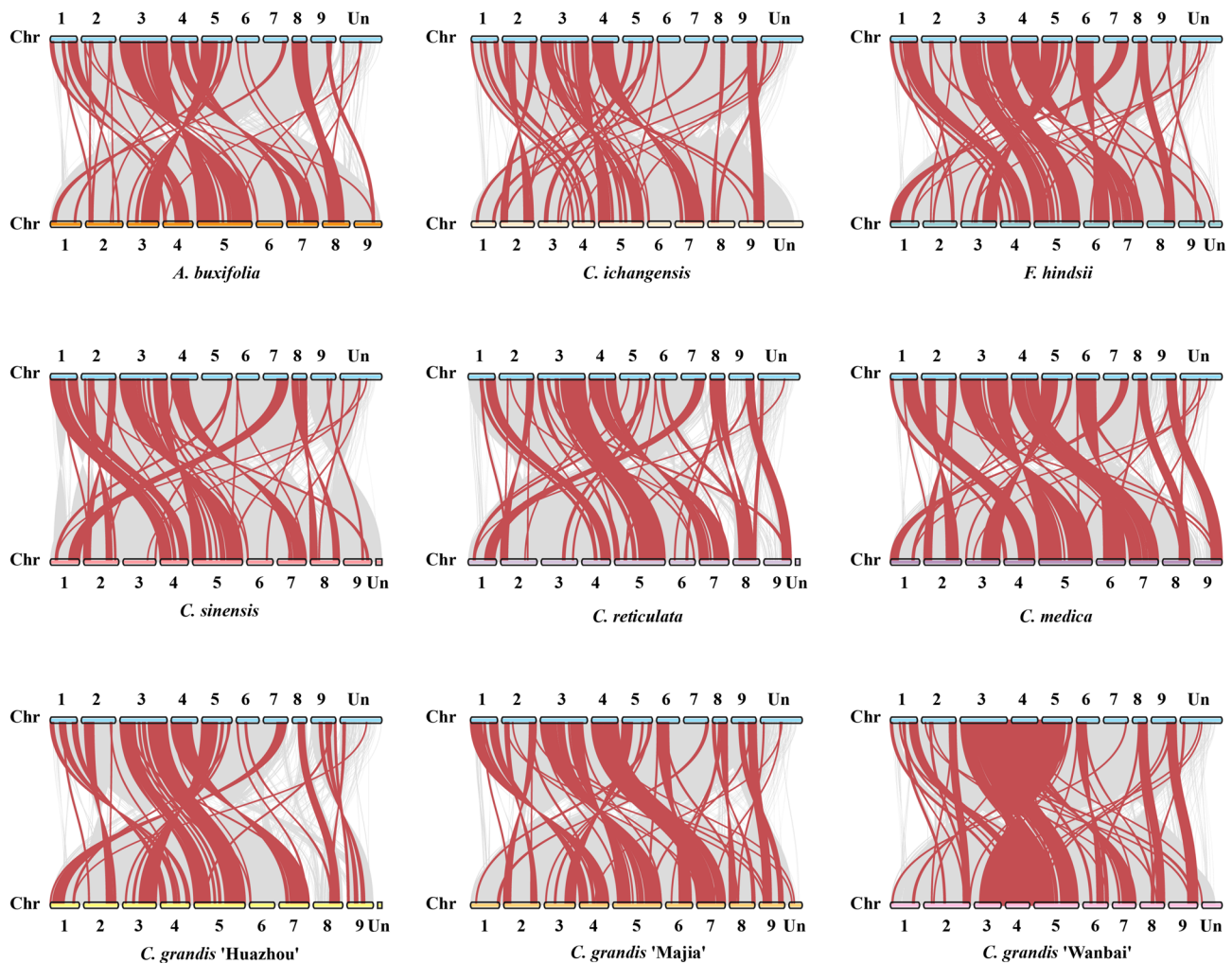


Fig. 7 Whole-genome collinearity analysis of the NACs between *P. trifoliata* and other citrus species. The synteny map displays the *P. trifoliata* genome in the upper section and corresponding citrus species genomes below. Gray curves connect indicate whole-genome collinear regions. Red curves connect conserved homologous regions containing NAC family genes. Un represents genes with uncertain chromosomal localization

grandis 'Hirado Buntan' vs. *C. ichangensis*, its homologous genes were increased 162.7-fold and 8.4-fold at 12 h post-cold treatment, respectively (Fig. 9D). In *P. trifoliata*, this gene increased 22.3-fold at 12 h, peaking to 85.84 folds after 72 h (Fig. 9E).

RT-qPCR validation confirmed its germplasm-specific expression: *P. trifoliata* showed 58.66-fold induction (control = 1.00) at 72 h, significantly exceeding *C. ichangensis* (15.97-fold), *C. grandis* 'Hirado Buntan' (12.40-fold), and *C. limon* (14.97-fold), with rapid response at 6 h (11.62-fold) (Fig. 9F). These findings reveal functional heterogeneity of NAC transcription factors in stress regulatory networks.

***PtrNAC2* negatively regulates cold tolerance**

In this study, virus-induced gene silencing was used to construct *PtrNAC2*-silenced lines (TRV2-*PtrNAC2*). RT-qPCR validation showed that the expression of this

gene was significantly reduced compared to the control (TRV2). After 12 h of -4 °C freezing treatment, phenotypic observations revealed severe wilting in TRV2 control leaves, while TRV2-*PtrNAC2* plants exhibited only minor damage (Fig. 10A). The *Fv/Fm* value of TRV2 plants dropped to 0.46 (a 42.3% decrease from pre-treatment levels), whereas TRV2-*PtrNAC2* retained a value of 0.68 (only a 15% decrease) (Fig. 10B-C). After cold treatment, the TRV2 plants showed an EL value of 25.92%, which was 2.57-fold higher than that of TRV2-*PtrNAC2* plants (10.08%) ($P < 0.001$) (Fig. 10D), demonstrating that silencing of this gene effectively alleviated cold-induced membrane damage. These results indicate that *PtrNAC2* plays a negative role in regulation of cold tolerance in *P. trifoliata*.

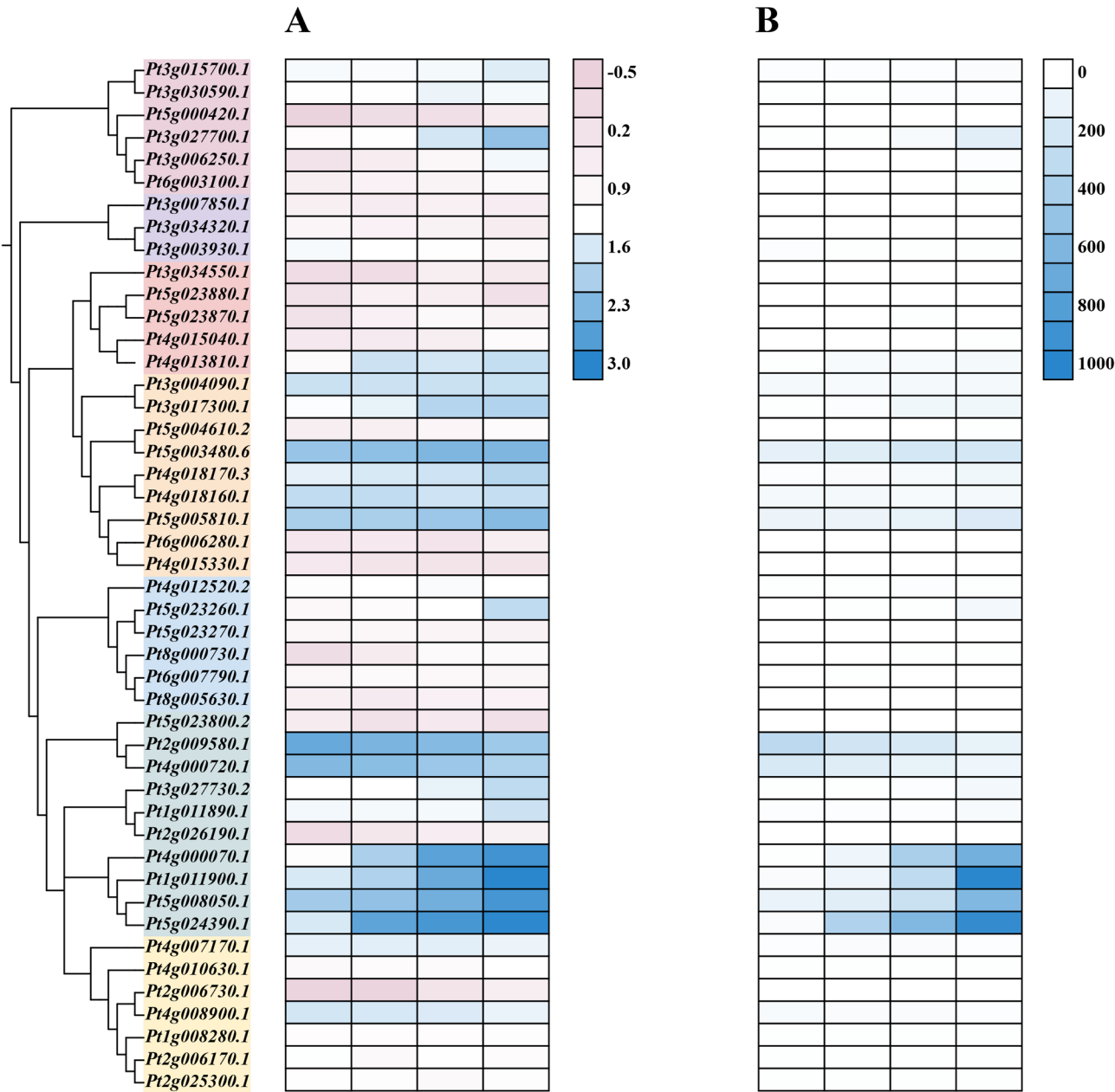


Fig. 8 Expression dynamics of *PtrNAC* genes under cold stress. **(A)** Heatmap of *PtrNAC* genes expression under cold stress (0 h, 6 h, 24 h, 72 h); **(B)** FPKM-based heatmap. The color gradient represents relative expression levels from low (light color) to high (dark color)

Discussion

This study systematically identified 135 *PtrNAC* genes in *P. trifoliata*, a cold-resistant model plant of citrus, revealing for the first time the unique evolutionary characteristics and low-temperature response regulatory network of the NAC transcription factor family in this species. With its scale ranking among the largest transcription factor families reported in citrus plants [66–70], this gene family provides novel insights into citrus genome evolution. Furthermore, the findings establish a systematic

analytical framework for investigating stress resistance mechanisms in perennial horticultural crops.

Chromosomal distribution and evolutionary dynamics

This study reveals a significant non-random distribution pattern of the *NAC* gene family in *P. trifoliata* at the chromosomal level. A total of 20 gene clusters were identified, with Chr3, Chr4, and Chr5 serving as primary reservoirs containing 57.78% of family members and 11 gene clusters. Notably, a 135.5-kb continuous cluster on Chr5 (*Pt5g023870*–*Pt5g023980*) harbors 10 members, while

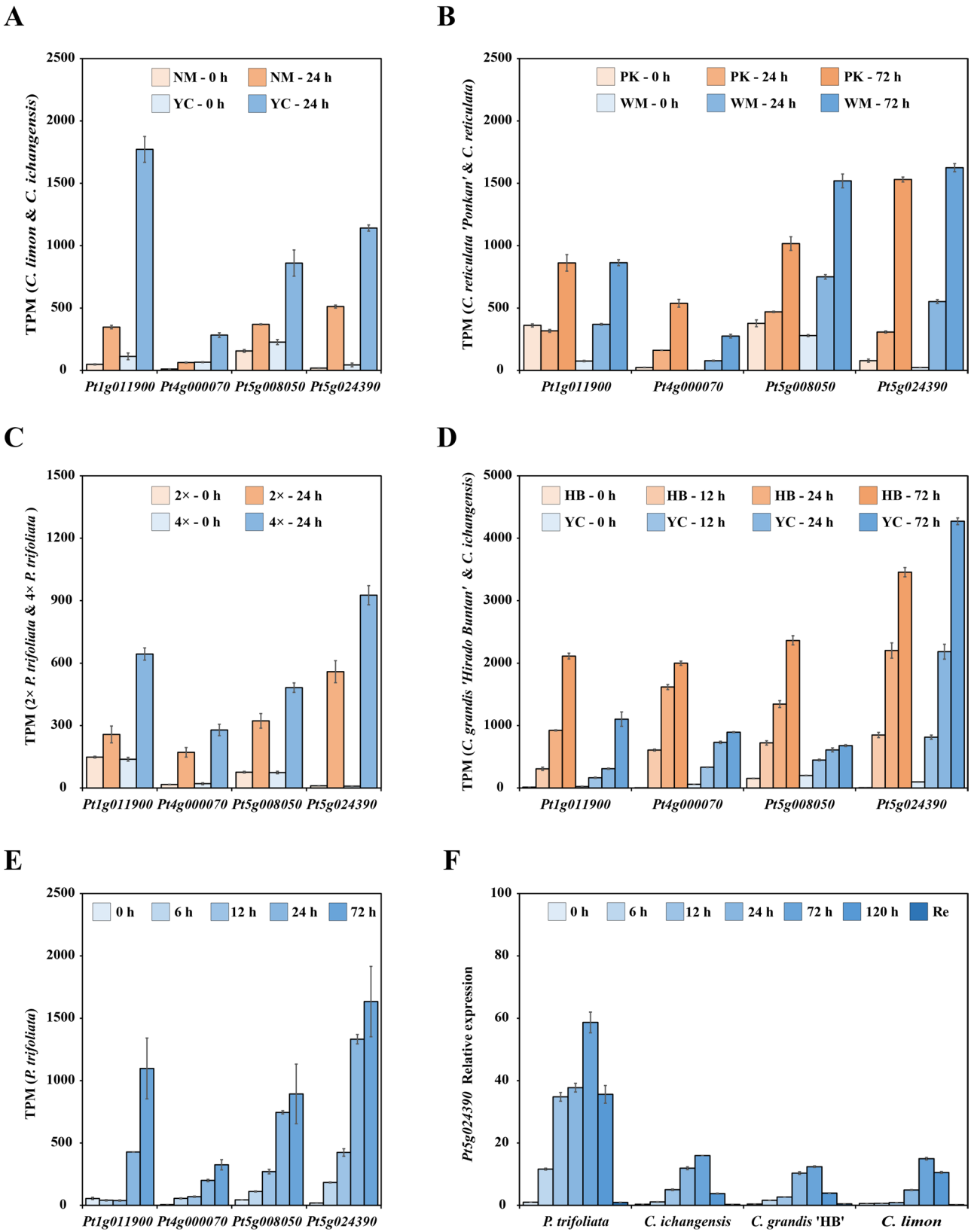


Fig. 9 (See legend on next page.)

(See figure on previous page.)

Fig. 9 Expression patterns of four cold-induced *PtrNAC* genes. **(A)** TPM (Transcripts Per Kilobase Million) of the genes in the transcriptome data of cold-treated *C. limon* (NM) and *C. ichangensis* (YC). **(B)** TPM of the genes in the transcriptome data of cold-treated *C. reticulata* 'Ponkan' (PK) and *C. reticulata* (WM). **(C)** TPM of the genes in the transcriptome data of cold-treated diploid (2x) and tetraploid (4x) *P. trifoliata*. **(D)** TPM of the genes in the transcriptome data of cold-treated *C. grandis* 'Hirado Buntan' (HB) and *C. ichangensis* (YC). **(E)** TPM of the genes in the transcriptome data of *P. trifoliata* under cold treatment at different time points. **(F)** RT-qPCR quantitative analysis of *NAC2* in *P. trifoliata*, *C. ichangensis*, *C. grandis* 'Hirado Buntan', and *C. limon*. RT-qPCR data are means \pm SD (n=3)

the smallest average inter-cluster distance (989 bp) on Chr2 indicates tandem duplication as the core expansion mechanism. The extreme variation in intergenic distances (714 bp to 38.4 kb) suggests multiple evolutionary mechanisms: compact clusters (e.g., Chr3/4/5) likely originate from recent tandem duplications, whereas dispersed clusters (e.g., Chr1/2) may result from recombination or insertional interference. The formation of these high-density gene clusters aligns with the rapid functional divergence patterns observed in gene families associated with both growth/development and stress response [71–74], where functionally critical genes form evolutionary hotspots through localized duplications and dynamically adjust cluster sizes via unequal recombination.

Gene duplication analysis demonstrates that proximal duplication (18.52% vs 9.05% genome-wide) and tandem duplication (19.96% vs 12.73% genome-wide) constitute primary expansion modes for the *PtrNAC* family. This differential duplication may drive functional specialization, contrasting sharply with the systemic gene contraction observed in *C. grandis* 'Huazhou' (63 genes) and *C. medica* (69 genes), likely resulting from selective gene loss during domestication. Importantly, the gene scarcity on Chr7/Chr8 may reflect ancestral chromosome loss or functional redundancy elimination, while three small clusters in unmapped regions (ChrUn) indicate persistent technical limitations in genome assembly (e.g., complex repeats or transposon-mediated gene migration).

Structural innovation and functional diversity

The high conservation of motifs 1–7 (gene coverage 64.4–96.3%) indicates their critical role in core functions, while the clade-specific distribution of motifs 8–10 (gene coverage 15.6–18.5%) may contribute to subfunctionalization. Similar architectural patterns were reported in sunflower *NAC* genes [31], where conserved N-terminal domains maintain DNA-binding capacity and variable C-terminal regions drive functional diversification, reflecting the coexistence of functional conservation and diversity. Phylogenetic analysis revealed distinct evolutionary clades in *P. trifoliata* Groups V–VII, combined with the identification of unconventional domains (e.g., KTI12, RRM_SF), elucidating functional innovation mechanisms in woody plant adaptation. The discovery of dual-NAM domain proteins (e.g., *Pt5g023900*) and peroxisome/cytoplasmic localization patterns challenges the conventional view of *NAC* proteins as strictly nuclear

transcription factors. These structural variations, potentially originating from gene duplication events [75], may enhance DNA-binding affinity and interaction complexity. The broad isoelectric point range and motif distribution collectively support functional diversity. Structural differentiation and subcellular localization patterns suggest neofunctionalization through domain fusion or post-translational regulation, mediating “moonlighting” roles in organelle signaling and membrane trafficking [76, 77]. Notably, such diversified patterns remain unreported in citrus *NAC* families [78], implying potential non-transcriptional regulatory functions. Analogous mechanisms were observed in rice: ONAC023 localizes to the cytoplasm under normal conditions but translocates to the nucleus with OsREM1.5 assistance during drought/heat stress, participating in transcriptional regulation and protein interactions [22].

Regulatory networks and evolutionary selection

Promoter *cis*-acting element analysis revealed that *PtrNAC* gene family members are precisely regulated by multi-layered transcriptional networks. Numerous hormone-responsive elements (including ABRE, TGA-element, GARE-motif) and stress-responsive elements (e.g., ARE, TC-rich repeats, WUN-motif) were identified, suggesting their potential involvement in environmental stress responses through integration of multiple signaling pathways. Notably, the widespread distribution of MYB and MYC elements further supports the crucial role of *NAC* genes in abiotic stress adaptation [79–81]. This “hormone-stress” co-regulatory module shows mechanistic parallels with the classical GA-BR signaling crosstalk observed in *A. thaliana* *JUB1* [16].

Collinearity analysis further revealed the evolutionary characteristics of this gene family: the majority of gene pairs exhibited signatures of purifying selection (K_a/K_s : 0.051–0.330), indicating strict conservation of their core functions during evolution. Notably, two gene pairs showed complete sequence identity, potentially resulting from recent duplication events or functional redundancy. This evolutionary pattern reflects a typical adaptive strategy in perennial horticultural crops, where purifying selection preserves essential functions, likely associated with their critical roles in plant growth and development or stress responses.

Domestication selection and polyploid advantage

Based on the phylogenetic tree construction of citrus species (consistent with [37]), we identified progressive gene dosage accumulation in the pummelo lineage. This phenomenon not only correlates with enhanced ecological adaptability but likely reflects human domestication selection pressure on agronomic traits such as fruit size and disease resistance, revealing directional reinforcement of gene functions through artificial selection. Further analysis demonstrated spatiotemporal specificity in gene dosage effects: under normal temperatures, tetraploid and diploid gene expression strictly follows the dosage conservation law (ratio $\approx 1:1$), whereas under cold stress, cold-responsive gene expression in tetraploid *P. trifoliata* increased by 2.15-fold compared to diploids. This elevation may be achieved through chromatin openness remodeling [82], which enhances transcriptional accessibility of key regulatory factors, thereby promoting their coordinated activation. The observed “stress-induced dosage-sensitive” regulatory pattern parallels the molecular mechanism by which the wheat *TaVRN1* gene modulates grain weight via dosage effects [83]. This model may provide a universal theoretical framework for understanding the ecological adaptability advantages of polyploid plants and offers novel insights for genetic improvement strategies in horticultural crops.

Functional heterogeneity

As core components of plant stress regulatory networks, transcription factors precisely control stress-responsive genes by specifically binding to promoter regions of target genes. These multi-layered regulatory mechanisms not only reshape plant metabolic networks and transcriptomic profiles, but also dynamically coordinate the balance between growth and stress tolerance through pathways such as RNA splicing and post-translational modifications [84–86].

In comparative transcriptomic analyses of *P. trifoliata* under cold stresses, the key gene *PtrNAC2* showed rapid response characteristics within 6 h of cold stress, with its conserved expression pattern potentially linked to interactions between promoter *cis*-acting elements and trans-regulatory factors. Notably, canonical cold-responsive NAC transcription factors generally improve plant cold tolerance through positive regulatory mechanisms. For instance: apple *MdNAC104* enhances cold resistance by coordinately activating both the CBF signaling pathway and anthocyanin/antioxidant metabolic pathways [25]; pepper *CaNAC064* mitigates oxidative damage through dual regulation of the antioxidant system and ROS metabolism [87]; banana *MaNAC1* reinforces cell wall integrity by upregulating cellulose synthase gene expression [88]. However, this study found that *PtrNAC2* exhibited the opposite biological function compared to

this traditional model: its silenced lines showed significantly enhanced cold tolerance under low-temperature stress. This discovery reveals a “transcriptional braking” mechanism opposing traditional positive regulation models [89, 90]. Further analysis revealed three key pathways underlying the *PtrNAC2* negative regulatory role: *PtrNAC2* directly suppresses transcriptional activation of cold-responsive target genes [91, 92]; it downregulates antioxidant enzyme genes, significantly reducing ROS scavenging capacity [93]; *PtrNAC2* disrupts CBF signaling by competitively binding to DNA or forming non-functional complexes with CBF regulators [94]. We hypothesize that the negative regulatory mechanism of *PtrNAC2* may involve the following molecular pathways: *PtrNAC2* retains a conserved N-terminal DNA-binding domain; however, its C-terminal region may occupy NAC-binding sites on cold-responsive gene promoters, physically blocking the binding of positive regulators to their targets. In rice, ONAC066 interacts with OsDJA6 to suppress MNAC3 activity [95]. This suggests *PtrNAC2* might form heterodimers with positive regulators, disrupting their nuclear localization or DNA-binding ability. These findings reveal a rare negative regulatory mode in the NAC family. Furthermore, they provide new insights into the complexity of plant stress adaptation mechanisms.

Conclusions

Based on the genome-wide analysis we identified a total of 135 *PtrNAC* genes in *P. trifoliata*, including 20 gene clusters. Most of the *NAC* genes are located in the three chromosomes. The *PtrNAC* genes may undergo proximal and tandem duplications for expansion. Collinearity analysis showed that 24.44% of the *PtrNAC* genes were retained in the homologous regions, and Ka/Ks ratio analysis further confirmed that purifying selection dominated their evolutionary process. Transcriptome landscapes revealed that several NAC genes were up-regulated by cold treatment, in which *Pt5g024390* (*PtrNAC2*) was most substantially induced. Virus-induced gene silencing indicated that *PtrNAC2* was a negative regulator of cold tolerance.

Taken together, we provide the global silhouette of NAC family genes in *P. trifoliata* and unveil several crucial members that may play a critical role in modulation of cold tolerance. The findings provide some valuable genes that may be engineered to generate cold-tolerant new germplasm in the future.

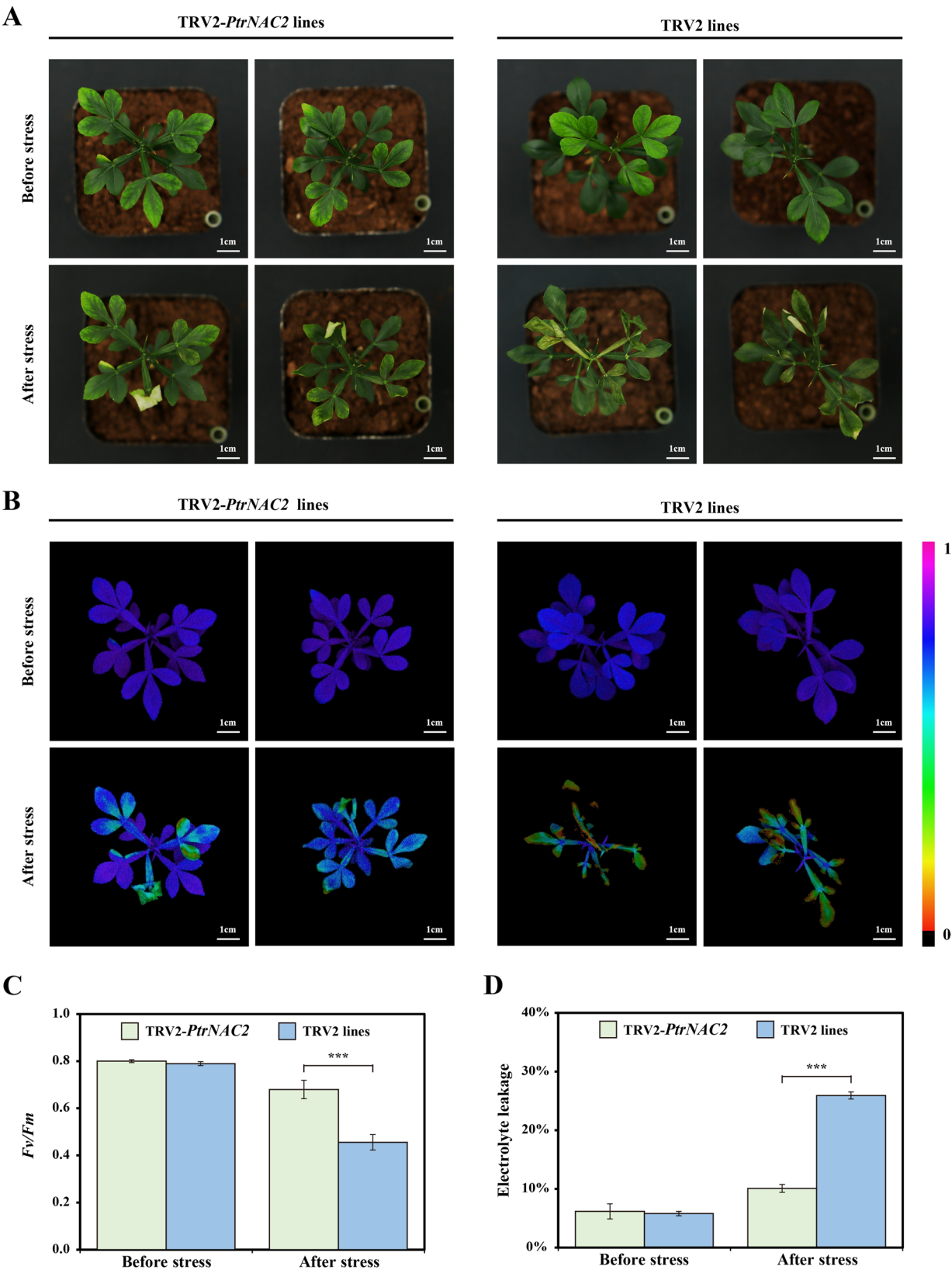


Fig. 10 Silencing *PtrNAC2* led to enhances cold tolerance in *P. trifoliata*. **(A)** Phenotypes of control (TRV2) and VIGS-treated (TRV2-PtrNAC2) plants before and after cold treatment. GFP fluorescence is shown. **(B)** Chlorophyll fluorescence imaging (pseudo-color scale from 0 to 1 is displayed adjacent to the images) and **(C)** F_v/F_m ratios. **(D)** Electrolyte leakage in tested lines before and after cold treatment. Error bars represent \pm SD ($n=3$). Asterisks indicate significant differences between control and VIGS lines under identical growth conditions ($***P < 0.001$). Scale bars = 1 cm

Supplementary Information

The online version contains supplementary material available at <https://doi.org/10.1186/s12870-025-06680-x>.

Supplementary Material 1

Acknowledgements

Not applicable.

Author contributions

T.F. and J.H.L. originated the research idea. T.F. performed the experiments. T.F., Y.W., H.W.C., P.X., Y.L.W. and X.J. analyzed the data. Y.W. and J.Q. offered guidance on drafting the manuscript. T.F. wrote the manuscript. C.L.L. and J.H.L. revised and finalized the writing. All authors reviewed the manuscript.

Funding

This work was supported by the Key Research and Development Program of Jiangsu Province (BE2023328), National Natural Science Foundation of China (32330095), and the National Key Research and Development Program of China (2022YFD1200503).

Data availability

No datasets were generated or analysed during the current study.

Declarations

Ethics approval and consent to participate

Not applicable.

Consent for publication

Not applicable.

Competing interests

The authors declare no competing interests.

Author details

¹National Key Laboratory for Germplasm Innovation & Utilization of Horticultural Crops, College of Horticulture and Forestry Sciences, Huazhong Agricultural University, Wuhan 430070, China

²Hubei Hongshan Laboratory, Wuhan 430070, China

Received: 3 April 2025 / Accepted: 5 May 2025

Published online: 14 May 2025

References

- Blauer R. Citrus. World Markets and Trade. United States Dep Agric Foreign Agric Serv. 2025.
- Vives-Peris V, Pérez-Clemente RM, Gómez-Cadenas A, López-Climent MF. Involvement of citrus shoots in response and tolerance to abiotic stress. *Hortic Adv*. 2024;2(1):1–11.
- Wang Y, Zuo L, Wei T, Zhang Y, Zhang Y, Ming R, et al. CHH methylation of genes associated with fatty acid and jasmonate biosynthesis contributes to cold tolerance in autotetraploids of *Poncirus trifoliata*. *J Integr Plant Biol*. 2022;64:2327–43.
- Curtolo M, de Souza Pacheco I, Boava LP, Takita MA, Granato LM, Galdeano DM, et al. Wide-ranging transcriptomic analysis of *Poncirus trifoliata*, *Citrus sunki*, *Citrus sinensis* and contrasting hybrids reveals HLB tolerance mechanisms. *Sci Rep*. 2020;10(1):1–14.
- Huang Y, Xu Y, Jiang X, Yu H, Jia H, Tan C et al. Genome of a citrus rootstock and global DNA demethylation caused by heterografting. *Hortic Res*. 2021;8(1):1–13.
- Dahro B, Li C, Liu J-H. Overlapping responses to multiple abiotic stresses in citrus: from mechanism Understanding to genetic improvement. *Hortic Adv*. 2023;1(1):1–19.
- Khan M, Dahro B, Wang Y, Wang M, Xiao W, Qu J, et al. The transcription factor ERF110 promotes cold tolerance by directly regulating sugar and sterol biosynthesis in citrus. *Plant J*. 2024;119(5):2385–401.
- Xiao W, Zhang Y, Wang Y, Zeng Y, Shang X, Meng L et al. The transcription factor TGA2 orchestrates Salicylic acid signal to regulate cold-induced proline accumulation in *Citrus*. *Plant Cell*. 2025;37(1):1–22.
- Ming R, Fang T, Ling W, Geng J, Qu J, Zhang Y et al. The GRAS transcription factor PtrPAT1 of *Poncirus trifoliata* functions in cold tolerance and modulates glycine betaine content by regulating the BADH-like gene. *Hortic Res*. 2025;12(1):1–12.
- Wu S, Hu C, Zhang S, Deng G, Sheng O, Dou T et al. Lipid metabolism and MAPK-ICE1 cascade play crucial roles in cold tolerance of banana. *Hortic Adv*. 2024;2(1):1–16.
- Olsen AN, Ernst HA, Leggio L, Lo, Skriver K. NAC transcription factors: structurally distinct, functionally diverse. *Trends Plant Sci*. 2005;10(2):79–87.
- Souer E, Van Houwelingen A, Kloos D, Mol J, Koes R. The *No apical meristem* gene of *Petunia* is required for pattern formation in embryos and flowers and is expressed at meristem and primordia boundaries. *Cell*. 1996;85(2):159–70.
- Xiong H, He H, Chang Y, Miao B, Liu Z, Wang Q, Dong F, Xiong L. Multiple roles of NAC transcription factors in plant development and stress responses. *J Integr Plant Biol*. 2025;00:1–29.
- Han K, Zhao Y, Sun Y, Li Y. NACs, generalist in plant life. *Plant Biotechnol J*. 2023;21(12):2433–57.
- Puranik S, Sahu PP, Srivastava PS, Prasad M. NAC proteins: regulation and role in stress tolerance. *Trends Plant Sci*. 2012;17(6):369–81.
- Shahnejat-Bushehri S, Tarkowska D, Sakuraba Y, Balazadeh S. *Arabidopsis* NAC transcription factor JUB1 regulates GA/BR metabolism and signalling. *Nat Plants*. 2016;2(3):1–9.
- Alshareef NO, Wang JY, Ali S, Al-Babili S, Tester M, Schmöckel SM. Overexpression of the NAC transcription factor *JUNGBRUNNEN1 (JUB1)* increases salinity tolerance in tomato. *Plant Physiol Biochem*. 2019;140:113–21.
- Zhang Z, Liu C, Li K, Li X, Xu M, Guo Y. CLE14 functions as a brake signal to suppress age-dependent and stress-induced leaf senescence by promoting JUB1-mediated ROS scavenging in *Arabidopsis*. *Mol Plant*. 2022;15(1):179–88.
- Li S, Yang JB, Li JQ, Huang J, Shen RF, Zeng DL, et al. A NAC transcription factor represses a module associated with Xyloglucan content and regulates aluminum tolerance. *Plant Physiol*. 2024;196(1):564–78.
- Tang W, Ye J, Yao X, Zhao P, Xuan W, Tian Y, et al. Genome-wide associated study identifies NAC42-activated nitrate transporter conferring high nitrogen use efficiency in rice. *Nat Commun*. 2019;10(1):1–11.
- Li R, Song Y, Wang X, Zheng C, Liu B, Zhang H, et al. OsNAC5 orchestrates OsAB15 to fine-tune cold tolerance in rice. *J Integr Plant Biol*. 2024;66(4):660–82.
- Chang Y, Fang Y, Liu J, Ye T, Li X, Tu H et al. Stress-induced nuclear translocation of ONAC203 improves drought and heat tolerance through multiple processes in rice. *Nat Commun*. 2024;15(1):1–21.
- Dong Y, Tang M, Huang Z, Song J, Xu J, Ahammed GJ, et al. The miR164a-NAM3 module confers cold tolerance by inducing ethylene production in tomato. *Plant J*. 2022;111(2):440–56.
- Wang J, Zheng C, Shao X, Hu Z, Li J, Wang P et al. Transcriptomic and genetic approaches reveal an essential role of the NAC transcription factor SINAP1 in the growth and defense response of tomato. *Hortic Res*. 2020;7(1):1–11.
- Mei C, Yang J, Mei Q, Jia D, Yan P, Feng B, et al. MdNAC104 positively regulates Apple cold tolerance via CBF-dependent and CBF-independent pathways. *Plant Biotechnol J*. 2023;21(10):2057–73.
- Wu H, Fu B, Sun P, Xiao C, Liu JH. A NAC transcription factor represses Putrescine biosynthesis and affects drought tolerance. *Plant Physiol*. 2016;172(3):1532–47.
- Zhu F, Luo T, Liu C, Wang Y, Zheng L, Xiao X, et al. A NAC transcription factor and its interaction protein hinder abscisic acid biosynthesis by synergistically repressing *NCED5* in *Citrus reticulata*. *J Exp Bot*. 2020;71(12):3613–25.
- Meng J, Sun S, Li A, Pan L, Duan W, Cui G, et al. A NAC transcription factor, PpNAC1, regulates the expression of *PpMYB10.1* to promote anthocyanin biosynthesis in the leaves of Peach trees in autumn. *Hortic Adv*. 2023;1(1):1–16.
- Ahmad M, Yan X, Li J, Yang Q, Jamil W, Teng Y, et al. Genome wide identification and predicted functional analyses of NAC transcription factors in Asian Pears. *BMC Plant Biol*. 2018;18(1):1–15.
- Jia D, Jiang Z, Fu H, Chen L, Liao G, He Y, et al. Genome-wide identification and comprehensive analysis of NAC family genes involved in fruit development in Kiwifruit (*Actinidia*). *BMC Plant Biol*. 2021;21(1):1–12.
- Li W, Zeng Y, Yin F, Wei R, Mao X. Genome-wide identification and comprehensive analysis of the NAC transcription factor family in sunflower during salt and drought stress. *Sci Rep*. 2021;11(1):1–12.

32. Liu S, Guan Y, Weng Y, Liao B, Tong L, Hao Z, et al. Genome-wide identification of the NAC gene family and its functional analysis in *Liriodendron*. BMC Plant Biol. 2023;23(1):1–19.
33. Wang Z, Chen Z, Wu Y, Mu M, Jiang J, Nie W, et al. Genome-wide identification and characterization of NAC transcription factor family members in *Trifolium pratense* and expression analysis under lead stress. BMC Genomics. 2024;25(1):1–15.
34. Liu H, Wang X, Liu S, Huang Y, Guo YX, Xie WZ, et al. Citrus Pan-Genome to breeding database (CPBD): A comprehensive genome database for citrus breeding. Mol Plant. 2022;15(10):1503–5.
35. Wang X, Xu Y, Zhang S, Cao L, Huang Y, Cheng J, et al. Genomic analyses of primitive, wild and cultivated citrus provide insights into asexual reproduction. Nat Genet. 2017;49:765–72.
36. Wang L, Huang Y, Liu ZA, He J, Jiang X, He F, et al. Somatic variations led to the selection of acidic and acidless orange cultivars. Nat Plants. 2021;7:954–65.
37. Huang Y, He J, Xu Y, Zheng W, Wang S, Chen P, et al. Pangenome analysis provides insight into the evolution of the orange subfamily and a key gene for citric acid accumulation in citrus fruits. Nat Genet. 2023;55:1964–75.
38. Feng D, Liu S, Chen M, Wang S, Xu M, Liu C, et al. Volatile content and genetic variation of Citron in Tibet and Yunnan. Plant Physiol. 2024;197:1–12.
39. Zheng W, Zhang W, Liu D, Yin M, Wang X, Wang S, et al. Evolution-guided multomics provide insights into the strengthening of bioactive flavone biosynthesis in medicinal Pummelo. Plant Biotechnol J. 2023;21:1577–89.
40. Lu Z, Huang Y, Mao S, Wu F, Liu Y, Mao X et al. The high-quality genome of Pummelo provides insights into the tissue-specific regulation of citric acid and anthocyanin during domestication. Hortic Res. 2022;9:1–10.
41. Zhu C, Zheng X, Huang Y, Ye J, Chen P, Zhang C, et al. Genome sequencing and CRISPR/Cas9 gene editing of an early flowering Mini-Citrus (*Fortunella hindsii*). Plant Biotechnol J. 2019;17:2199–210.
42. Liu S, Xu Y, Yang K, Huang Y, Lu Z, Chen S et al. Origin and de Novo domestication of sweet orange. Nat Genet. 2025;57:754–62.
43. Nordberg H, Cantor M, Dusheyko S, Hua S, Poliakov A, Shabalov I, et al. The genome portal of the department of energy joint genome institute: 2014 updates. Nucleic Acids Res. 2014;42(D1):D26–31.
44. Jin J, Tian F, Yang DC, Meng YQ, Kong L, Luo J, et al. PlantTFDB 4.0: toward a central hub for transcription factors and regulatory interactions in plants. Nucleic Acids Res. 2017;45(D1):D1040–5.
45. Reiser L, Bakker E, Subramaniam S, Chen X, Sawant S, Khosa K, et al. The Arabidopsis information resource in 2024. Genetics. 2024;227(1):1–11.
46. Mistry J, Chuguransky S, Williams L, Qureshi M, Salazar GA, Sonnhammer ELL, et al. Pfam: the protein families database in 2021. Nucleic Acids Res. 2021;49(D1):D412–9.
47. Potter SC, Luciani A, Eddy SR, Park Y, Lopez R, Finn RD. HMMER web server: 2018 update. Nucleic Acids Res. 2018;46(W1):W200–4.
48. Letunic I, Khedkar S, Bork P, SMART. Recent updates, new developments and status in 2020. Nucleic Acids Res. 2021;49(D1):D458–60.
49. Osorio D, Rondón-Villareal P, Torres R, Peptides. A package for data mining of antimicrobial peptides. R J. 2015;7(1):4–14.
50. Horton P, Park KJ, Obayashi T, Fujita N, Harada H, Adams-Collier CJ, et al. WoLF PSORT: protein localization predictor. Nucleic Acids Res. 2007;35:585–7.
51. Edgar RC. MUSCLE: multiple sequence alignment with high accuracy and high throughput. Nucleic Acids Res. 2004;32(5):1792–7.
52. Nguyen LT, Schmidt HA, Von Haeseler A, Minh BQ. IQ-TREE: A fast and effective stochastic algorithm for estimating maximum-likelihood phylogenies. Mol Biol Evol. 2015;32(1):268–74.
53. Stamatakis A. RAxML version 8: A tool for phylogenetic analysis and post-analysis of large phylogenies. Bioinformatics. 2014;30(9):1312–3.
54. Letunic I, Bork P. Interactive tree of life (iTOL): an online tool for phylogenetic tree display and annotation. Bioinformatics. 2007;23(1):127–8.
55. Lescot M, Déhais P, Thijs G, Marchal K, Moreau Y, Van De Peer Y, et al. PlantCARE, a database of plant *cis*-acting regulatory elements and a portal to tools for *in Silico* analysis of promoter sequences. Nucleic Acids Res. 2002;30(1):325–7.
56. Hu B, Jin J, Guo AY, Zhang H, Luo J, Gao G. GSDS 2.0: an upgraded gene feature visualization server. Bioinformatics. 2015;31(8):1296–7.
57. Wang Y, Tang H, Debarry JD, Tan X, Li J, Wang X, et al. MCScanX: A toolkit for detection and evolutionary analysis of gene synteny and collinearity. Nucleic Acids Res. 2012;40(7):1–14.
58. Krzywinski M, Schein J, Birol I, Connors J, Gascoyne R, Horsman D, et al. Circos: an information aesthetic for comparative genomics. Genome Res. 2009;19(9):1639–45.
59. Chao J, Li Z, Sun Y, Aluko OO, Wu X, Wang Q, et al. MG2C: a user-friendly online tool for drawing genetic maps. Mol Hortic. 2021;1(1):1–4.
60. Zhang Z, Li J, Zhao XQ, Wang J, Wong GKS, Yu J. KaKs_Calculator: calculating Ka and Ks through model selection and model averaging. Genomics Proteom Bioinforma. 2006;4(4):259–63.
61. Livak KJ, Schmittgen TD. Analysis of relative gene expression data using Real-Time quantitative PCR and the $2^{-\Delta\Delta C_T}$ method. Methods. 2001;25(4):402–8.
62. Dai W, Wang M, Gong X, Liu JH. The transcription factor FcWRKY40 of *Fortunella crassifolia* functions positively in salt tolerance through modulation of ion homeostasis and proline biosynthesis by directly regulating SOS2 and P5CS1 homologs. New Phytol. 2018;219(3):972–89.
63. Zhang Y, Zhu J, Khan M, Wang Y, Xiao W, Fang T, et al. Transcription factors ABF4 and ABR1 synergistically regulate amylase-mediated starch catabolism in drought tolerance. Plant Physiol. 2023;191(1):591–609.
64. Dähro B, Wang Y, Khan M, Zhang Y, Fang T, Ming R, et al. Two AT-Hook proteins regulate *A/NIN7* expression to modulate sucrose catabolism for cold tolerance in *Poncirus trifoliata*. New Phytol. 2022;235(6):2331–49.
65. Zaman NK, Abdullah MY, Othman S, Zaman NK. Growth and physiological performance of aerobic and lowland rice as affected by water stress at selected growth stages. Rice Sci. 2018;25(2):82–93.
66. Liu DH, Luo Y, Han H, Liu YZ, Alam SM, Zhao HX, et al. Genome-wide analysis of citrus TCP transcription factors and their responses to abiotic stresses. BMC Plant Biol. 2022;22(1):1–14.
67. Dai WS, Peng T, Wang M, Liu JH. Genome-wide identification and comparative expression profiling of the WRKY transcription factor family in two *Citrus* species with different *Candidatus Liberibacter Asiaticus* susceptibility. BMC Plant Biol. 2023;23(1):1–18.
68. Fu MK, He YN, Yang XY, Tang X, Wang M, Dai WS. Genome-wide identification of the GRF family in sweet orange (*Citrus sinensis*) and functional analysis of the *CsGRF04* in response to multiple abiotic stresses. BMC Genomics. 2024;25(1):1–16.
69. Qu J, Xiao P, Zhao ZQ, Wang YL, Zeng YK, Zeng X, et al. Genome-wide identification, expression analysis of WRKY transcription factors in *Citrus ichangensis* and functional validation of *CiWRKY31* in response to cold stress. BMC Plant Biol. 2024;24(1):1–17.
70. Yin T, Xu R, Zhu L, Yang X, Zhang M, Li X, et al. Comparative analysis of the *PAL* gene family in nine citrus species provides new insights into the stress resistance mechanism of *Citrus* species. BMC Genomics. 2024;25(1):1–23.
71. Leister D. Tandem gene duplication drives the rapid evolution of disease resistance genes in plants. Trends Genet. 2004;20(3):113–6.
72. Krsticevic FJ, Arce DP, Ezpeleta J, Tapia E. Tandem duplication events in the expansion of the small heat shock protein gene family in *Solanum lycopersicum* (cv. Heinz 1706). G3 genes. Genomes Genet. 2016;6(10):3027–34.
73. Jiang X, Assis R. Rapid functional divergence after small-scale gene duplication in grasses. BMC Evol Biol. 2019;19(1):1–11.
74. Zhao J, Guo R, Guo C, Hou H, Wang X, Gao H. Evolutionary and expression analyses of the Apple basic leucine zipper transcription factor family. Front Plant Sci. 2016;7:1–13.
75. Diao P, Chen C, Zhang Y, Meng Q, Lv W, Ma N. The role of NAC transcription factor in plant cold response. Plant Signal Behav. 2020;15(9):1–10.
76. Jeffery CJ. Protein moonlighting: what is it, and why is it important? Philos Trans R Soc Lond B Biol Sci. 2018;373(1738):1–8.
77. Singh N, Bhalla N. Moonlighting proteins. Annu Rev Genet. 2020;54:265–85.
78. de Oliveira TM, Cidade LC, Gesteira AS, Filho MAC, Filho WSS, Costa MGC. Analysis of the NAC transcription factor gene family in citrus reveals a novel member involved in multiple abiotic stress responses. Tree Genet Genomes. 2011;7(6):1123–34.
79. Erpen L, Devi HS, Grosser JW, Dutt M. Potential use of the DREB/ERF, MYB, NAC and WRKY transcription factors to improve abiotic and biotic stress in Transgenic plants. Plant Cell Tiss Org. 2018;132(1):1–25.
80. Wang X, Niu Y, Zheng Y. Multiple functions of Myb transcription factors in abiotic stress responses. Int J Mol Sci. 2021;22(1):1–14.
81. Li Z, Huang Y, Shen Z, Wu M, Huang M, Hong SB et al. Advances in functional studies of plant MYC transcription factors. Theor Appl Genet. 2024;137:1–62.
82. Zhang H, Zheng R, Wang Y, Zhang Y, Hong P, Fang Y, et al. The effects of *Arabidopsis* genome duplication on the chromatin organization and transcriptional regulation. Nucleic Acids Res. 2019;47(15):7857–69.
83. Yu Z, Cui B, Xiao J, Jiao W, Wang H, Wang Z, et al. Dosage effect genes modulate grain development in synthesized *Triticum durum*-*Haynaldia villosa* allohexaploid. J Genet Genomics. 2024;51(10):1089–100.
84. Zhu JK. Abiotic stress signaling and responses in plants. Cell. 2016;167(2):313–24.

85. Ding Y, Yang S. Surviving and thriving: how plants perceive and respond to temperature stress. *Dev Cell*. 2022;57(8):947–58.
86. Zhang H, Zhu J, Gong Z, Zhu JK. Abiotic stress responses in plants. *Nat Rev Genet*. 2022;23(2):104–19.
87. Hou X, ming, Zhang H feng, Liu S ya, Wang X ke, Zhang Ymeng, Meng Y et al. cheng,. The NAC transcription factor *CaNAC064* is a regulator of cold stress tolerance in peppers. *Plant Sci*. 2020;291:1–10.
88. Yin Q, Qin W, Zhou Z, Wu AM, Deng W, Li Z, et al. Banana MaNAC1 activates secondary cell wall cellulose biosynthesis to enhance chilling resistance in fruit. *Plant Biotechnol J*. 2024;22(2):413–26.
89. Cai J, Panda S, Kazachkova Y, Amzallag E, Li Z, Meir S et al. A NAC triad modulates plant immunity by negatively regulating *N*-hydroxy pipecolic acid biosynthesis. *Nat Commun*. 2024;15(1):1–16.
90. Zhang J, Lyu H, Chen J, Cao X, Du R, Ma L et al. Releasing a sugar brake generates sweeter tomato without yield penalty. *Nature*. 2024;635:647–56.
91. Yue Q, Xie Y, Yang X, Zhang Y, Li Z, Liu Y, et al. An indel variant in the promoter of the NAC transcription factor *MdNAC18.1* plays a major role in Apple fruit ripening. *Plant Cell*. 2025;37:1–18.
92. Zhong Q, Yu J, Wu Y, Yao X, Mao C, Meng X, et al. Rice transcription factor OsNAC2 maintains the homeostasis of immune responses to bacterial blight. *Plant Physiol*. 2024;195:785–98.
93. Niu MX, Feng CH, He F, Zhang H, Bao Y, Liu SJ, et al. The miR6445-*NAC029* module regulates drought tolerance by regulating the expression of glutathione S-transferase U23 and reactive oxygen species scavenging in *Populus*. *New Phytol*. 2024;242:2043–58.
94. Wang T, Ma X, Chen Y, Wang C, Xia Z, Liu Z, et al. SINAC3 suppresses cold tolerance in tomatoes by enhancing ethylene biosynthesis. *Plant Cell Environ*. 2024;47:3132–46.
95. Wang H, Bi Y, Yan Y, Yuan X, Gao Y, Noman M, et al. A NAC transcription factor MNAC3-centered regulatory network negatively modulates rice immunity against blast disease. *J Integr Plant Biol*. 2024;66:2017–41.

Publisher's note

Springer Nature remains neutral with regard to jurisdictional claims in published maps and institutional affiliations.